Supporting Information

Wang et al. 10.1073/pnas.1300126110

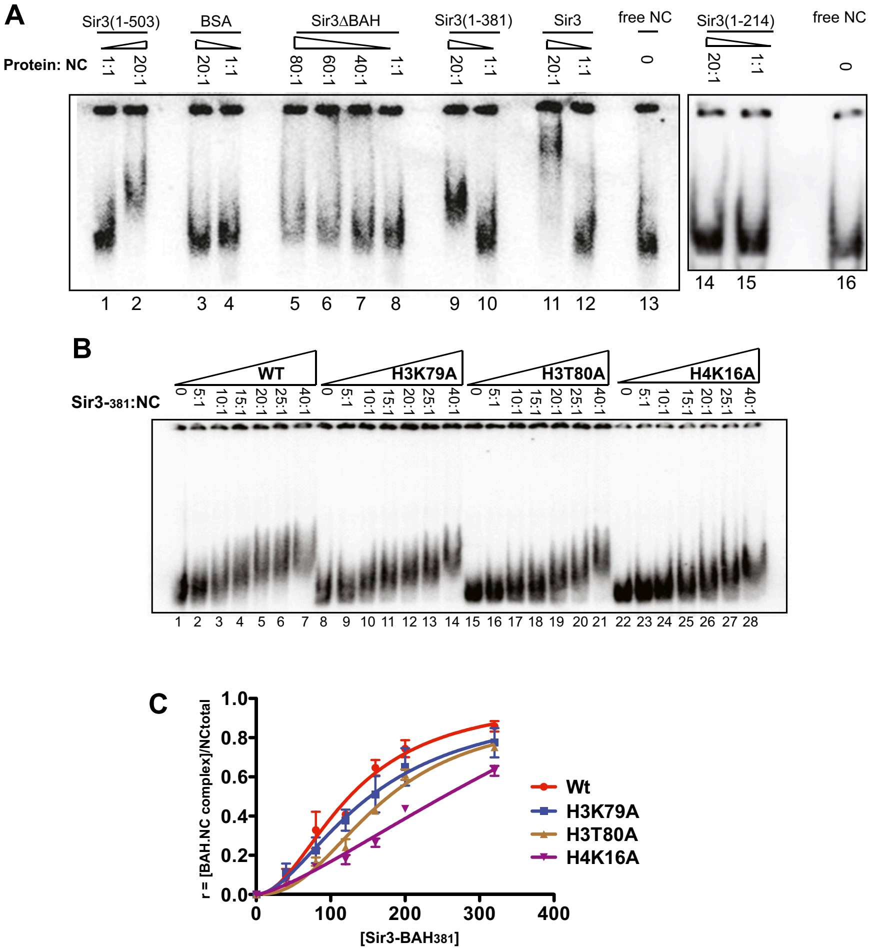

(kD values: wt, 126 nM; K79A, 152 nM; T80A, 167 nM; K16A, 637 nM)

Fig. S1. Nucleosome binding properties of silent information regulator 3 (Sir3)-381 and other Sir3 fragments. (*A*) Gel-shift assays examining the association of full-length Sir3 and the indicated Sir3 subfragments with yeast mononucleosomes (NC). Mononucleosomes were reconstituted using bacterially expressed yeast histones and a ^{32}P-labeled 601 DNA fragment (1). Sir3 protein was purified from yeast as described previously (1). (*B*) Gel-shift assays testing the association of Sir3-381 protein with nucleosomes containing WT, H3K79A, H3T80A, or H4K16A histones. (*C*) Band intensities were quantified by analysis of phosphorimager data with Quantity 1 software to generate binding curves for three independent experiments and calculate binding constant (K_D) values. Data were fit with the binding equation $y = A * \frac{[P]^h}{[P]^h + K^h} + B$, where *h* is the Hill coefficient, [*P*] is the protein concentration, *K* is the K_D, and *A* and *B* are scaling parameters (2).

1. Johnson A, et al. (2009) Reconstitution of heterochromatin-dependent transcriptional gene silencing. *Mol Cell* 35(6):769–781.
2. Tanner NA, et al. (2008) Single-molecule studies of fork dynamics in *Escherichia coli* DNA replication. *Nat Struct Mol Biol* 15(2):170–176.

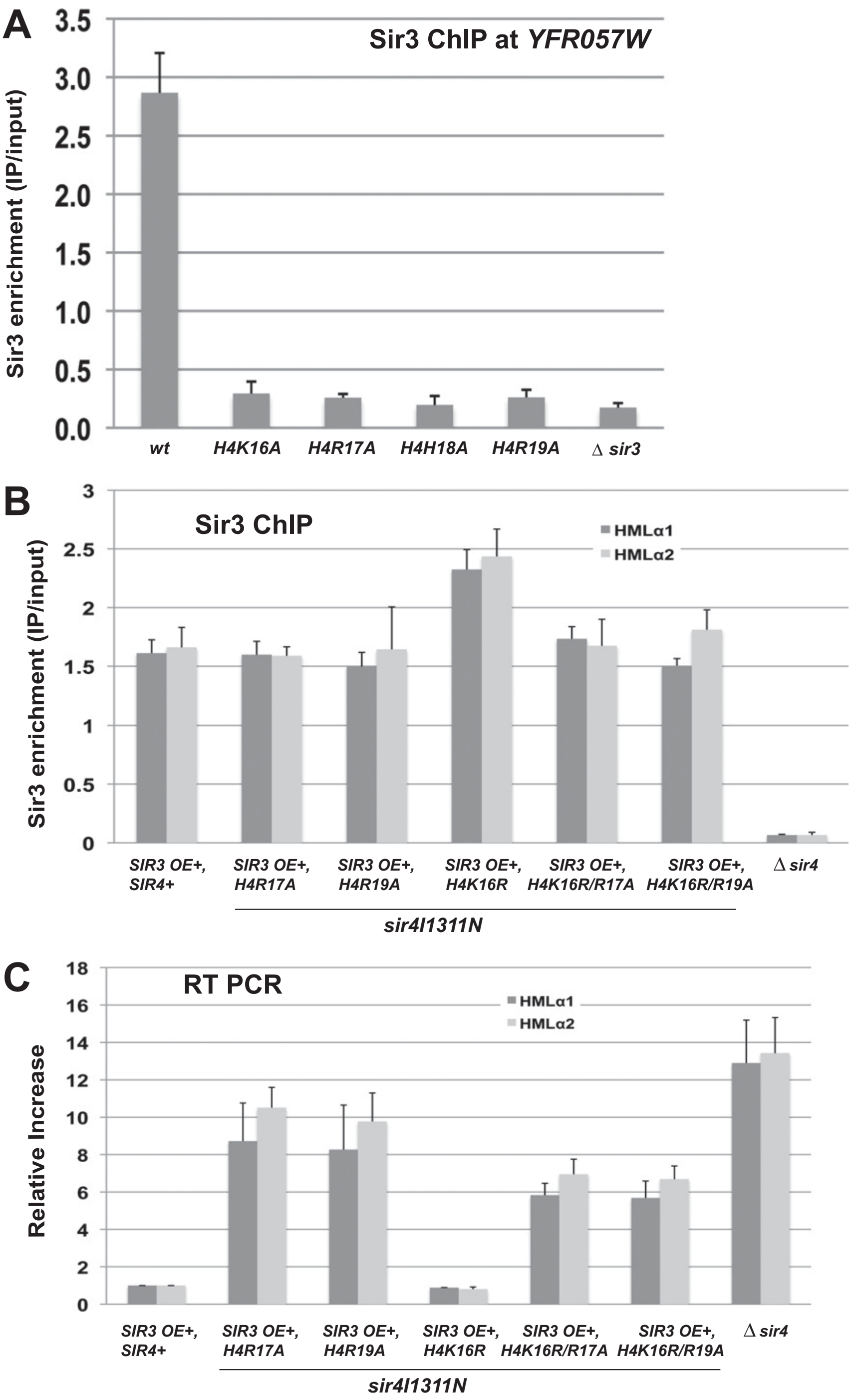

Fig. S2. The effect of histone H4R17 and R19 substitutions on the association of Sir3 with the subtelomeric *YFR057W* gene and the *homothalic left* (*HML*) locus. (*A*) Quantitative ChIP experiments showing the association of Sir3 with a subtelomeric open reading frame on the right arm of chromosome VI (*YFR057w*) in WT, *sir3Δ*, or cells carrying the indicated histone H4 substitutions. Error bars represent SDs. (*B*) Quantitative ChIP experiments showing that in cells carrying histone H4R17A or R19A substitutions, alone or in combination with H4K16R substitutions, Sir3 can bind to the *HMLα1* and *α2* genes. The binding of overexpressed Sir3 (Sir3OE) occurs independent of its interaction with Sir4, because the *sir4I1311N* mutation abolishes the Sir3–Sir4 interaction. Error bars represent SDs. (*C*) Quantitative RT-PCR assays showing *HMLα1* and *α2* gene expression in H4KR17A and R19A cells. Mutation of H4K16, but not of either H4R17A or R19A, to arginine, which mimics the deacetylated state, suppressed the silencing defect of *sir4I1311* mutation. Error bars represent SDs.

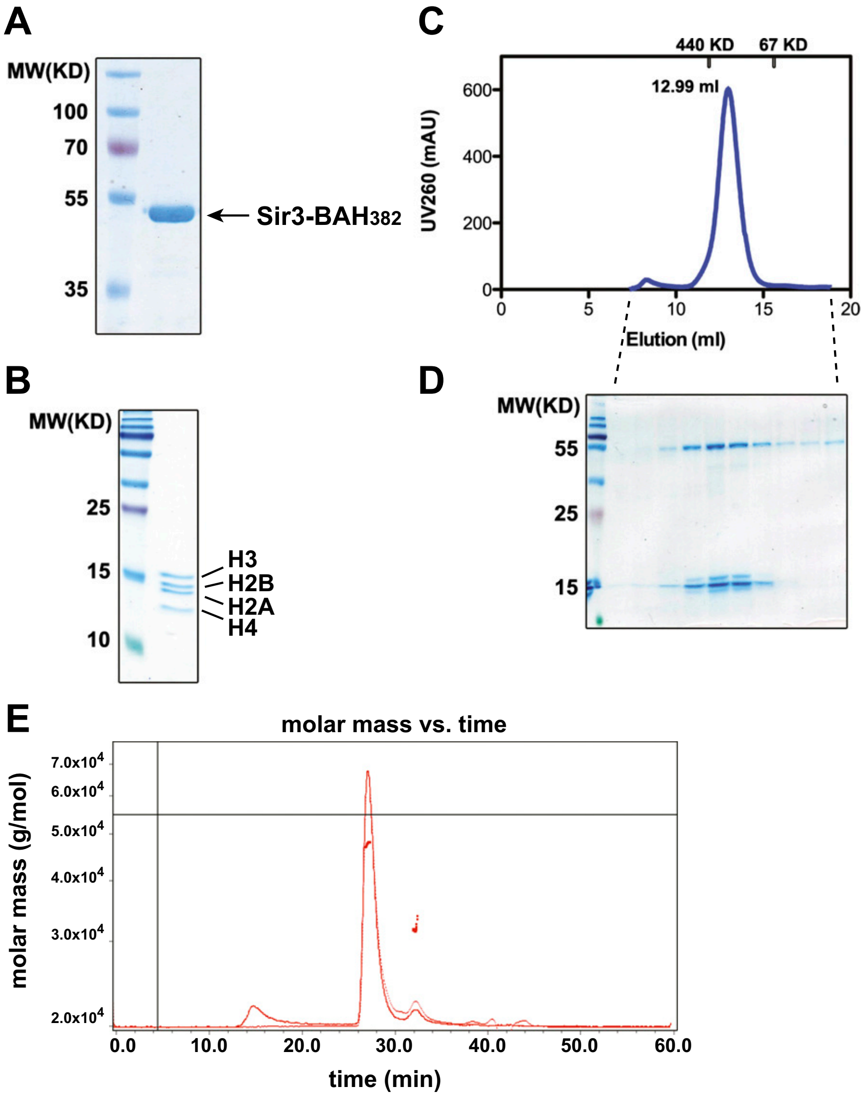

Fig. S3. Sir3-382 purification and characterization. (*A* and *B*) Coomassie blue-stained gels of purified Sir3-382 (*A*) and the yeast histone octamer (*B*). (*C* and *D*) Gel filtration profiles of the Sir3-382–nucleosome complex detected by UV absorbance at 260 nm (*C*) and staining with Coomassie blue (*D*), which show comigration of Sir3-382 and the nucleosome. (*E*) Multiangle light scattering experiment showing that the BAH domain elutes from the gel filtration column at a molecular mass predicted for a monomeric 43,510-Da protein.

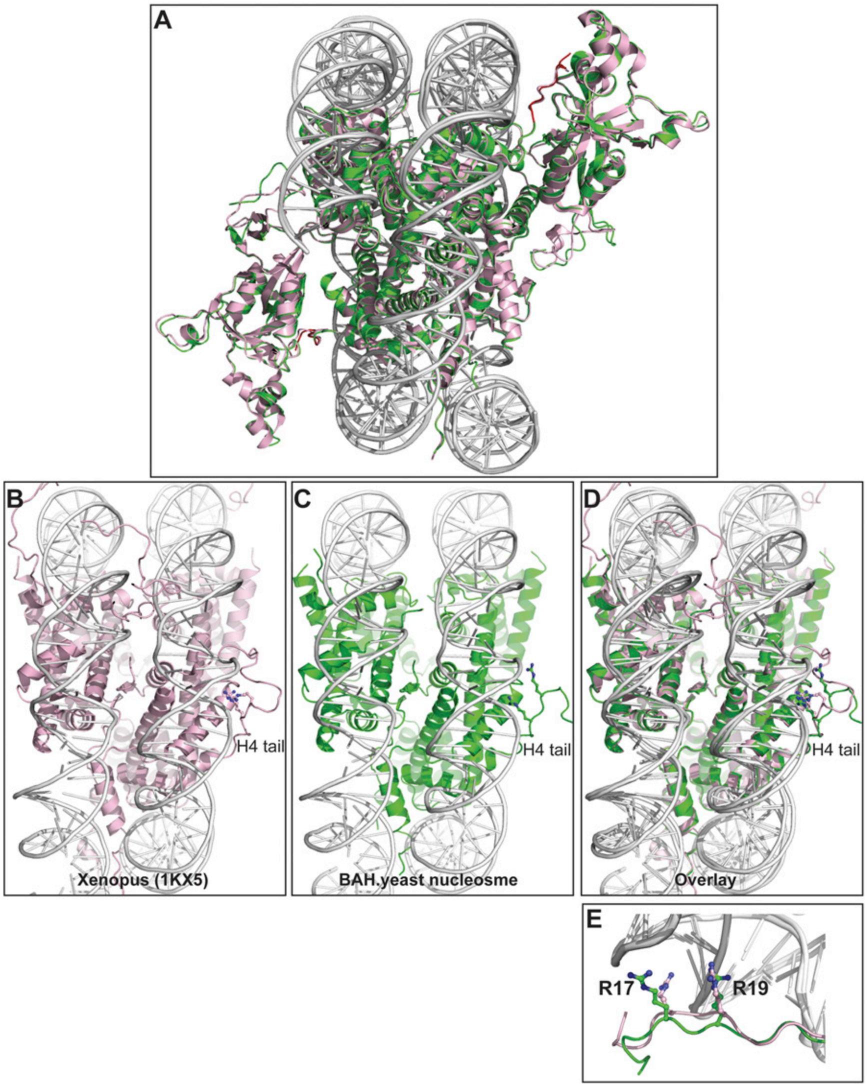

Fig. S4. Overlays of the Sir3-BAH–yeast nucleosome with other nucleosome structures. (*A*) Overlays of the Sir3-BAH–yeast nucleosome (green, this study) and Sir3-BAH–*Xenopus* nucleosome (pink) complexes (1). (*B*) Free *Xenopus* nucleosome crystal structure (1KX5) (2). (*C*) Structure of Sir3-BAH.yeast nucleosome with the BAH atoms removed. (*D* and *E*) Overlays of the structures in *B* and *C* showing that one of the two histone H4 chains in the free *Xenopus* nucleosome structure adopts a conformation similar to that observed in the Sir3-BAH–yeast nucleosome structure. However, in the free *Xenopus* nucleosome structure, H4R17 points into the minor groove and is not within DNA-bonding distance (zoom-in view in *E*).

1. Armache KJ, Garlick JD, Canzio D, Narlikar GJ, Kingston RE (2011) Structural basis of silencing: Sir3 BAH domain in complex with a nucleosome at 3.0 Å resolution. *Science* 334(6058): 977–982.
2. Davey CA, Sargent DF, Luger K, Maeder AW, Richmond TJ (2002) Solvent- mediated interactions in the structure of the nucleosome core particle at 1.9 Å resolution. *J Mol Biol* 319(5): 1097–1113.

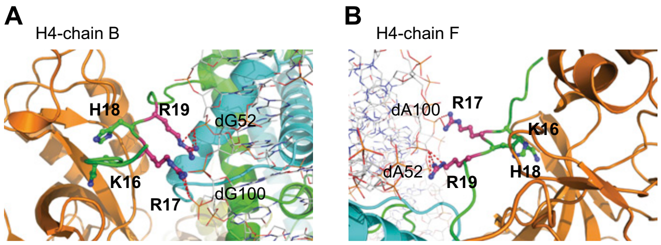

Fig. S5. Interaction of H4 with nucleosomal DNA in the Sir3-BAH–yeast nucleosome complex. H4R17 and R19 in both H4 chain B (*A*) and chain F (*B*) can engage in similar interactions with the phosphates of nucleotides 52 and 100 across minor grooves on opposite DNA strands on the two sides of the nucleosome.

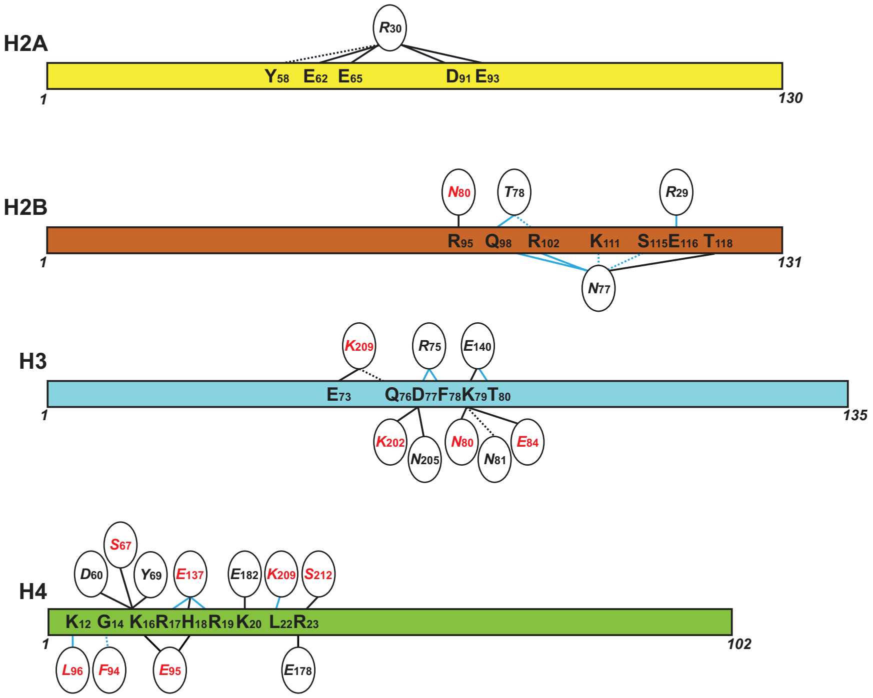

Fig. S6. Summary of the main interaction sites between Sir3-BAH382 and each of the four histones mapped onto the primary structure of the histones. Solid lines denote strong interactions (bond distances <4 Å), and dotted lines denote weaker interactions (bond distances 4–5 Å). Blue lines denote interactions between side chains in Sir3-BAH with the carbonyl atoms of the indicated amino acids in histones. The residues identified in previous mutagenesis studies with critical roles in silencing or Sir3 binding are shown in red.

Table S1. ***Saccharomyces cerevisiae*** **strains used in this study**

Name	Genotype	Reference
SF1	JRY2334, Mata ade2-1 can1-100 his3-11 leu2-3.112 trp1 ura3-1 GAL	J. Rine
DMY2376	SF1 pep4Δ::LEU2	(1)
DMY3628	DMY2376 SIR3-TAP-K.I-TRP1	(1)
DMY3810	DMY2376 SIR3BAH-TAP-K.I-TRP1	This study
DMY3863	DMY2376 SIR3ΔBAH-TAP-K.I-TRP1	(2)
WZY42	Mat a ura3-52 lys2-801 ade2-1–1 trp1Δ63 his3Δ200 leu2Δ1 hht1-hhf1::pWZ405-F2F9-LEU2, hht2-hhf2::pWZ403-F4F10-HIS3 Ycp50-copyII (HHT2-HHF2)	(3)
DMY3903	WZY42 Sir3-TAP-KAN	(2)
DMY3985	WZY42 Sir3BAH-TAP-KAN	(2)
SF10	BJ5459, Mat a ura3-52 trp1 lys2-801 leu2Δ1 his3Δ200 pep4ΔHIS prb1Δ1.6R can1 GAL	E. Jones
ADR2973	JRY2334, Mat a ade2-1 can1-100 his3-11 leu2-3.112 trp1 ura3-1 GAL	(1)
JDY135	Mat a His3Δ200 leu2Δ1 lys2Δ0 met15Δ0 trp1Δ63 ura3-167 ade2::HISG hht1-hhf1::NAT hht2-hhf2-HYG RDN1::TY1-MET15 TELV::ADE2 (HHT1-HHF1) CEN-URA3	(4)

1. Rudner AD, Hall BE, Ellenberger T, Moazed D (2005) A nonhistone protein–protein interaction required for assembly of the SIR complex and silent chromatin. *Mol Cell Biol* 25(11): 4514–4528.
2. Onishi M, Liou GG, Buchberger JR, Walz T, Moazed D (2007) Role of the conserved Sir3-BAH domain in nucleosome binding and silent chromatin assembly. *Mol Cell* 28(6):1015–1028.
3. Zhang W, Bone JR, Edmondson DG, Turner BM, Roth SY (1998) Essential and redundant functions of histone acetylation revealed by mutation of target lysines and loss of the Gcn5p acetyltransferase. *EMBO J* 17(11):3155–3167.
4. Dai J, et al. (2008) Probing nucleosome function: A highly versatile library of synthetic histone H3 and H4mutants. *Cell* 134(6):1066–1078.

Table S2. Plasmids used in this study

Description	Plasmid	Source
pRS414 CEN TRP1 H3K56A	Boeke-EMH-H3-56|K56A	(1)
pRS414 CEN TRP1 H4K16Q	pWZ414-F25 (pDM 688)	(2)
pRS414 CEN TRP1 H4K16A	Boeke-EMH-H4-16|K16A	(1)
pRS414 CEN TRP1 H4R17A	Boeke-EMH-H4-17|R17A	(1)
pRS414 CEN TRP1 H4H18A	Boeke-EMH-H4-18|H18A	(1)
pRS414 CEN TRP1 H4R19A	Boeke-EMH-H4-19|R19A	(1)
pRS414 CEN TRP1 H4K20A	Boeke-EMH-H4-20|K20A	(1)
pDM1009	Sir3-3XFLAG, Gal 1–10, 2u (pRS425)	(3)
pDM1082	pRET3a-H3K79A (SC histone mutant)	(4)
pDM1084	pRET3a-H4K16A (SC histone mutant)	(4)
pDM1230	pRET3a-H3T80A (SC histone mutant)	This study
pDM1091	601 nucleosome-positioning sequence (Amp^R)	(5)

1. Dai J, et al. (2008) Probing nucleosome function: A highly versatile library of synthetic histone H3 and H4 mutants. *Cell* 134(6):1066–1078.
2. Zhang W, Bone JR, Edmondson DG, Turner BM, Roth SY (1998) Essential and redundant functions of histone acetylation revealed by mutation of target lysines and loss of the Gcn5p acetyltransferase. *EMBO J* 17(11):3155–3167.
3. Buchberger JR, et al. (2008) Sir3–nucleosome interactions in spreading of silent chromatin in *Saccharomyces cerevisiae*. *Mol Cell Biol* 28(22):6903–6918.
4. Johnson A, et al. (2009) Reconstitution of heterochromatin-dependent transcriptional gene silencing. *Mol Cell* 35(6):769–781.
5. Li G, Widom J (2004) Nucleosomes facilitate their own invasion. *Nat Struct Mol Biol* 11(8):763–769.

Table S3. Crystallographic data collection and refinement statistics for Sir3-382–*Sc*NCP

Data collection	
Space group	$P6_1$
Cell dimensions	
A, *b*, *c*, Å	103.682, 103.682, 556.378
α, β, γ, °	90, 90, 120
Wavelength, Å	0.97920
Resolution, Å	139.09–3.09
R_{merge} (high-resolution shell), %	3.9 (48.7)
I/σ (high-resolution cell)	14.0 (1.5)
Completeness (high-resolution shell), %	97.4 (97.9)
Redundancy (high-resolution shell)	2.9 (2.9)
Refinement	
Resolution, Å	85.45–3.09
No. of reflections	59,664
$R_{work/}$ R_{free}, %	23.13/25.48
B-factors, Å^2	
Overall	78.24
Protein	52.14
DNA	118.55
rms deviations	
Bond lengths, Å	0.002
Bond angles, °	0.611
Ramachandran plot*	
Most favored and additional allowed, %	99.9
Generously allowed, %	0.1
Disallowed, %	0

*Calculated in the ADIT Validation Server (http://deposit.rcsb.org/adit/).